

Mechanism for coupling between properties of interfaces and bulk semiconductors

Kapil Dev, M. Y. L. Jung, R. Gunawan, R. D. Braatz, and E. G. Seebauer*

Department of Chemical Engineering, University of Illinois, Urbana, Illinois 61801, USA

(Received 14 February 2003; revised manuscript received 8 July 2003; published 18 November 2003)

A mechanism is described by which interface electronic properties can affect bulk semiconductor behavior. In particular, experimental measurements by photoreflectance of Si(100)-SiO₂ interfaces show how a controllable degree of band bending can be introduced near the interface by ion bombardment and annealing. The resulting electric field near the interface can affect dopant concentration profiles deep within the semiconductor bulk by drastically changing the effective interfacial boundary condition for annihilation of charged interstitial atoms formed during bombardment. Kinetic measurements of band-bending evolution during annealing show that the bending persists for substantial periods even above 1000 °C. Unusually low activation energies for the evolution point to a distribution of energies for healing of bombardment-generated interface defects. The findings have significant implications for *p-n* junction formation during complementary metal oxide semiconductor device processing.

DOI: 10.1103/PhysRevB.68.195311

PACS number(s): 73.20.-r, 61.72.Cc, 68.35.-p, 78.40.Fy

I. INTRODUCTION

Comparing the physics of bulk solids with that of free surfaces or solid interfaces has long occupied substantial research effort. Curiously, much less attention has focused upon the direct coupling between these phenomena. Although there is a significant literature concerning the coupling between surface and bulk magnetization,¹⁻³ the remaining papers are scattered thinly among a variety of applications, including nematic liquid crystal ordering at solid interfaces,⁴ bulk quenching of surface exciton emission,⁵ bulk-influenced surface state behavior at steps on metals,⁶ and bulk doping effects on surface band bending in semiconductors.⁷ This last paper treats the effects of the semiconductor bulk on surface electronic properties. However, given the capacity of bulk semiconductors to support space charge, the reverse influence is also plausible—namely, that surface and interface electronic properties affect bulk semiconductor behavior. The present work offers evidence for such effects by demonstrating how a controllable degree of band bending can be introduced at a semiconductor-oxide interface by ion bombardment and annealing, and outlines a mechanism by which the resulting space charge can affect dopant diffusion deep within the semiconductor bulk. The findings have significant implications for *p-n* junction formation during conventional complementary metal oxide semiconductor (CMOS) device processing of transistors. The results also offer insights into the nature of defect healing at semiconductor-oxide interfaces at temperatures much higher than those explored previously in the literature.

It is well known that the Si-SiO₂ interface can be prepared remarkably free of electrically active defects. Bond rupture by ion bombardment at energies of a few hundred electron volts should be capable of creating controlled amounts of such defects, although we are aware of no published literature regarding the possibility. If bond breakage at the interface resembles that at a free Si surface, as few as 10¹² defects/cm² (i.e., a fractional interface coverage of 0.01 to 0.001) can induce pinning of the interface Fermi level⁸ in the

rough vicinity of midgap.⁹ For bulk material with substantial doping, such pinning would lead to band bending in the underlying Si on the order of 0.5 V. The corresponding electric field near the interface would rise to levels sufficiently high to perturb the dielectric constant at optical frequencies¹⁰ and thereby be detectable by optical methods.

We exploited this phenomenon to measure with photoreflectance the degree of band bending at the Si-SiO₂ interface after ion bombardment. Photoreflectance (PR) is one of a class of modulation spectroscopies in which a semiconductor is periodically perturbed, and the resulting change in dielectric constant is detected by reflectance.^{11,12} PR accomplishes the modulation with a chopped laser beam having $h\nu$ greater than the fundamental band-gap energy E_g . Photogenerated minority carriers migrate to the interface and recombine with charge stored there. The resulting change in built-in field affects the surface reflectance R in narrow regions of wavelength corresponding to optical transitions of the substrate material. The small reflectance change $\Delta R/R$ exhibits a spectral dependence that is monitored with a weaker, independent probe beam using phase-sensitive detection. The presence of a nonzero PR spectrum demonstrates unequivocally the existence of surface band bending, and experiments as a function of temperature and pump intensity can yield useful estimates of the degree of this band bending.¹³

II. EXPERIMENT

Experiments were performed in a small turbomolecularly pumped ultrahigh vacuum chamber set up in conjunction with optics for PR as described elsewhere for a similar system.¹² Such systems are typically capable of base pressures in the low-10⁻⁹-torr range. The chamber was equipped with a variable energy ion gun (up to 2.0 keV) for ion implantation. Samples of dimensions 1.2 cm × 1.0 cm were cut from boron-doped Si(100) wafers with resistivity of 0.014 Ω cm corresponding to a doping level of 1 × 10¹⁸ cm⁻³. In experiments requiring PR measurements as a function of temperature, resistive heating was employed, with temperature monitored by a chromel-alumel thermocouple. A

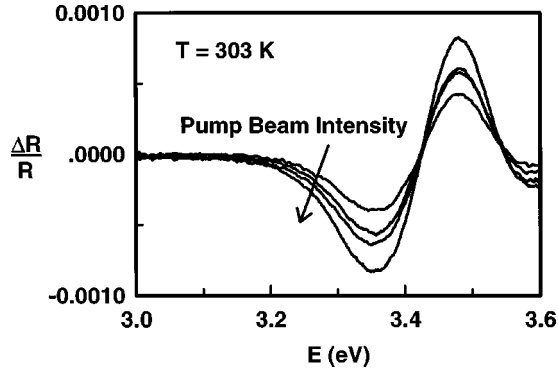


FIG. 1. Series of raw PR spectra from Ar-implanted Si(100)-SiO₂ for different pump beam intensities. Presence of a nonzero amplitude signifies band bending.

1000-W Xe arc lamp was used for rapid (75 °C/s) heating during kinetic measurements, with temperature monitored by an optical pyrometer. A He-Ne laser operating at 632 nm served as the pump beam. Spectra were collected in the vicinity of the nearly degenerate E_1 and E'_0 (Ref. 14) optical transitions of Si, which lie near 3.4 eV.

PR spectra from the free Si(100) surface were obtained by removing native oxide with aqueous HF, quickly transferring the sample to the vacuum chamber, baking to achieve ultra-high vacuum, and heating the surface at 800 °C for 2 min. Independent experiments in our laboratory with Auger spectroscopy have shown that this procedure yields an oxide-free surface.¹⁵ Oxidized surfaces were formed by exposure to 7 mbar of O₂ for 15 min at 940 °C. Published oxidation kinetics¹⁶ indicate that oxide thickness from this procedure should be 2.0 nm. After oxidation, samples were implanted with 0.5-keV Ar ions. We used Ar to induce interface bond breakage without significantly affecting the doping level of the underlying Si, which affects both the amplitude and the line shape of the PR spectra and therefore complicates data interpretation. Fluences ranged up to 1×10^{15} cm⁻².

III. RESULTS AND DISCUSSION

A. Existence and magnitude of band bending at the implanted interface

Figure 1 shows room-temperature PR spectra at various illumination intensities for samples implanted with 1×10^{15} cm⁻² Ar ions. The nonzero spectral amplitude ($\Delta R/R \sim 10^{-3}$) in the figure demonstrates the existence of band bending at the interface. An ion fluence study revealed zero amplitude below roughly 1×10^{11} ions/cm². In the range from 1×10^{11} to 1×10^{13} ions/cm², spectral amplitude increased monotonically with no change in the line shape. Above 1.2×10^{13} ions/cm² this amplitude progression continued, but the entire spectrum shifted downward slightly in energy (~ 0.03 eV) with no other change in shape. Above 1×10^{15} ions/cm², the amplitude, shape, and position all remained unchanged.

To quantify the magnitude of the band bending, we used a procedure detailed elsewhere.¹³ Briefly, the PR spectrum was fitted to the classic third-derivative functional form expected

for electromodulation spectroscopies of this type at optical transitions far from the fundamental band gap:¹⁰

$$\Delta R/R = \text{Re}[C e^{i\phi} (E - E_{\text{crit}} + i\Gamma)^{-n}], \quad (1)$$

where C denotes an amplitude factor, ϕ is a phase factor, Γ is a broadening parameter, and E_{crit} and n are the energy and dimension of the critical point associated with the transition. As mentioned earlier, there are actually two optical transitions in the region of the measurements: the E_1 and E'_0 . These transitions of Si are nearly degenerate, however, being separated by less than 0.1 eV.¹⁴ Elsewhere,¹³ we have shown that the resulting spectra can be adequately fit by a single line shape having the form of Eq. (1) with the parameter n chosen phenomenologically to be 3. The remaining parameters can then be extracted from the experimental spectra according to the methods outlined in Ref. 10. With the assumption of full depletion in the space-charge region (and negligible tunneling through this 25-nm-wide layer), the amplitude factor C scales linearly with the photoinduced change in surface potential,^{17,18} which in turn varies logarithmically with the photocurrent.^{19,20} It can then be shown¹³ that C obeys

$$C = A_1 \ln[A_2 I \exp(V_s/kT) + 1], \quad (2)$$

where k denotes Boltzmann's constant, T the temperature, I the pump beam intensity, and V_s the surface potential referenced to flat band. A_1 and A_2 represent constants describing optical properties of the substrate. Variation of C with I at constant T yields the composite parameter $A_2 \exp(V_s/kT)$. An Arrhenius plot of $A_2 \exp(V_s/kT)$ at different temperatures yields V_s .

There is a mean electric field assumption that tacitly underlies this analysis; that is, it is assumed that a space-charge region is well defined and uniform everywhere on the specimen surface. It may be asked whether this assumption properly applies in the presence of the high doping concentrations (1×10^{18} cm⁻³) and possible charge compensation induced by ion-generated defects in our specimens. Indeed, Lu *et al.*²¹ have shown that at carrier concentrations significantly above 10^{18} cm⁻³ in GaAs, the PR signal at the E_0 transition disappears. This phenomenon was attributed to spatial fluctuations in effective surface depletion depth; random variations in the spacing of dopant atoms become comparable to the depth of the space-charge region, which broadens the PR spectra into unobservability. At lower concentrations, however, these workers found that a mean-field line shape description worked adequately.

It has also been shown that the E_1 line shape for GaAs changes at carrier concentrations between 1×10^{17} and 1.5×10^{18} cm⁻³.²² Very substantial dopant compensation was known to be present at the highest carrier concentrations. Nevertheless, the functional form of Eq. (1) still adequately fit the PR data. Changes in Γ were attributed to dopant-induced spectral broadening, presumably due to increased carrier scattering. Changes in ϕ were attributed primarily to variations in electric field strength over the penetration depth of the probe light.

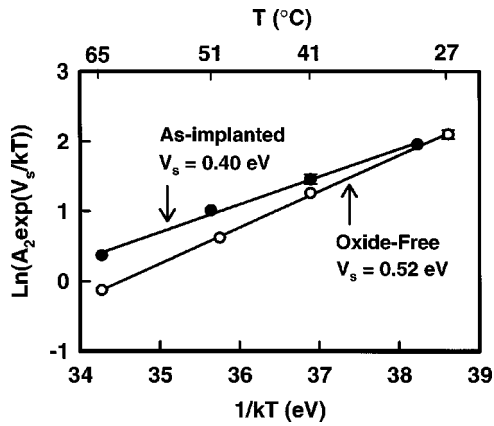


FIG. 2. Arrhenius plots of the quantity $A_2 \exp(V_s/kT)$ for oxide-free Si(100) and oxidized, Ar-implanted Si(100).

Fujimoto *et al.*²³ have similarly encountered no difficulty in using Eq. (1) for Si doped to levels comparable to ours. Their material was not damaged by implantation the way ours was, but we have found by comparing PR signals from unimplanted, atomically clean Si and implanted, oxidized Si that the PR line shape does not change significantly. Based on these various lines of evidence, we conclude that the mean-field assumption is adequate.

Figure 2 shows Arrhenius plots connected with Eq. (2) for clean Si(100) and for oxidized, Ar-implanted material; V_s equals 0.52 ± 0.01 and 0.40 ± 0.02 eV for the respective surfaces. The value for clean Si(100) is higher than that of 0.33 eV obtained by Fujimoto *et al.*²³ by a similar method for *n*-type Si(100) with a similar doping level. We note, however, that although the surfaces in Ref. 23 were nominally free of adsorbate, the precise degree of cleanliness cannot be ascertained from the reported data. Photoemission results for clean Si(100) exist but have weaknesses. Himpsel *et al.*²⁴ reported that E_F on undoped Si(100)-(2×1) lies 0.34 eV above the valence-band maximum based on core-level photoelectron emission at room temperature. However, they based this result on an early value for $E_F - E_{\text{VBM}}$ of 0.33 eV reported by Allen and Gobeli²⁵ for a different surface—cleaved Si(111)-(2×1). Himpsel *et al.*²⁶ subsequently made improved measurements on Si(111)-(2×1) to yield 0.40 eV. Thus, the earlier result for Si(100)-(2×1) must be readjusted to 0.41 eV. This result lies within about 0.1 eV of our result, which is rather close given varying crystal faces and doping levels employed in the relevant literature.

B. Annealing behavior of band bending: Distribution of activation energies

After implantation, specimens were annealed isothermally under vacuum for various times and temperatures. All PR spectra were collected at 300 K after quenching because the signal for Si becomes quite small above 150 °C (Ref. 13) due to substantial thermal generation of charge carriers. Annealing studies revealed that band bending remained nonzero for several minutes of annealing up to temperatures of at least 940 °C (the limit of our apparatus). Two distinct kinetics regimes characterize the evolution of band bending. Between

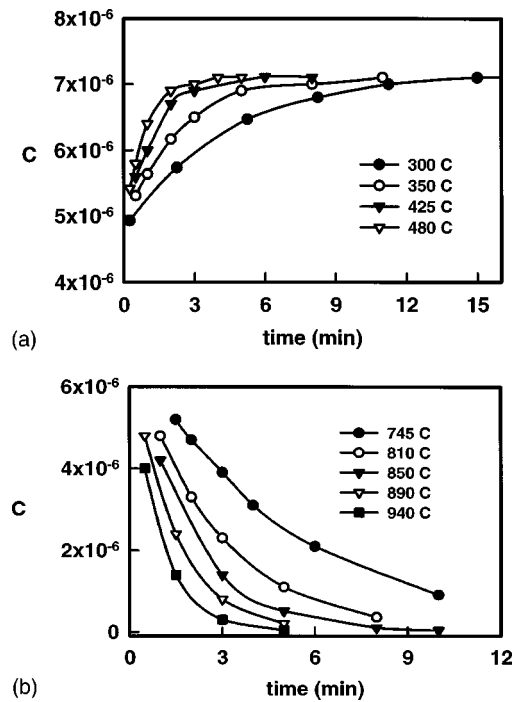


FIG. 3. Variation of spectral amplitude C with time for Ar-implanted Si(100) annealed at different temperatures in the (a) low- T regime and (b) in the high- T regime. Lines are guides to the eye. In (a), a saturation value C_{sat} is reached at long times.

roughly 300 and 500 °C, the pinning amplitude C increases to a saturation value C_{sat} (corresponding to a band bending of 0.56 eV). Above roughly 750 °C, C decreases to zero. The variation of amplitude C with time in the two regimes appears in Figs. 3(a) and 3(b). The rate constants describing the evolution of C obey simple first-order kinetics in both regimes as shown in Figs. 4(a) and 4(b). Arrhenius plots describing the temperature dependence of the two rate constants appear in Fig. 5. In the low-temperature regime, the rate constant k_{low} obeys $(2.4 \times 10^{1 \pm 0.1} \text{ min}^{-1}) \exp(-0.20 \pm 0.02 \text{ eV}/kT)$. The corresponding high-temperature rate constant k_{high} obeys $(4.9 \times 10^{3 \pm 0.1} \text{ min}^{-1}) \exp(-0.89 \pm 0.02 \text{ eV}/kT)$.

The transformations in both regimes take place at temperatures higher than those characterizing other defects known to exist at the Si-SiO₂ interface. For example, emission and capture of charge carriers by interface traps in metal oxide semiconductor (MOS) structures takes place at roughly 200 K.²⁷ So-called P_b centers correspond to Si dangling bonds at the Si(111)-SiO₂ (Ref. 28) and Si(100)-SiO₂ (Ref. 29) interfaces. Formation of these defects³⁰ and reaction with molecular hydrogen^{31,32} take place at lower temperatures and have activation energies greatly different from ours.

The activation energies we obtain for k_{low} and k_{high} fall far below the values expected for first-order reactions in the respective temperature regimes. With “normal” preexponential factors near 10^{13} s^{-1} , the respective activation energies would be roughly 1.8 and 2.9 eV at 400 and 800 °C, respectively. Large-scale free-surface reconstructions for Si(111) and GaAs(100) exhibit similarly low values.¹² However, ion fluences of only $1 \times 10^{11} \text{ ions/cm}^2$ (equivalent to roughly

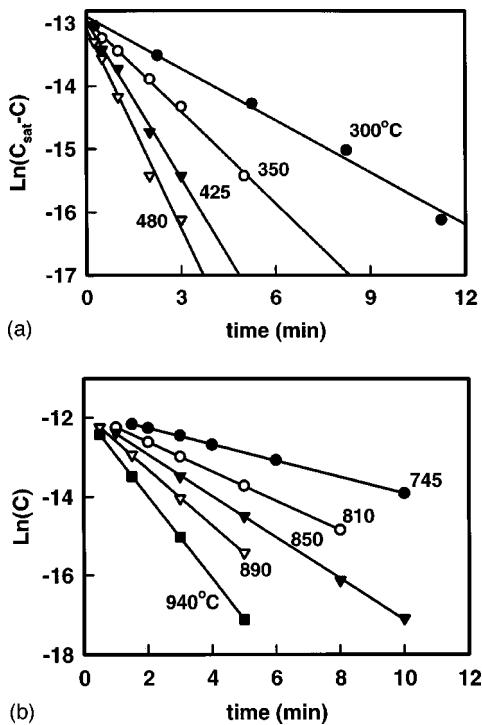


FIG. 4. C vs time data fit to first-order kinetics for (a) the low- T regime and (b) the high- T regime. Lines are the least-square fits. In (a), C_{sat} is the saturation value of C in Fig. 3(a).

0.01% of a monolayer) are required to initiate band bending. This fact suggests that point defects govern the kinetics rather than large-scale rearrangements. Bulk diffusion of point defects or atomic reactants also cannot explain the results. Activation energies for hopping of such species through both Si (Ref. 37) and SiO_2 (Ref. 33) tend to be 1 eV or less. With normal hopping prefactors on the order of $10^{-3} \text{ cm}^2/\text{s}$, the diffusion lengths would be too long to be rate limiting.

We consider it more likely that the kinetics reflect healing by local rearrangements of defects having a wide variety of geometries, leading to a wide and possibly continuous distribution of activation energies. Studies of P_b centers indicate

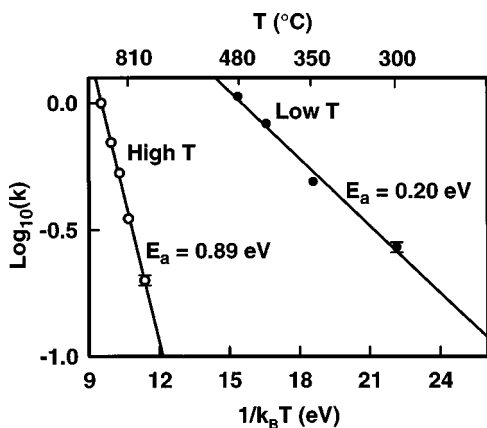


FIG. 5. Arrhenius plots of rate constants describing evolution of band bending.

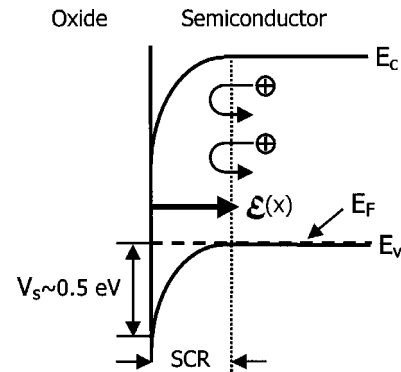


FIG. 6. Schematic band diagram for a p -type semiconductor showing the reflection of positively charged interstitial atoms by the electric field $E(x)$ within the space-charge region (SCR) near the oxide interface.

that the defected Si-SiO_2 interface supports silicon atoms in various oxidation states ranging from +1 through +4.³⁴ Indeed, the density of suboxide states (lower than +4) appears to vary in proportion to P_b center density for interfaces of SiO_2 with both $\text{Si}(100)$ and $\text{Si}(111)$.³⁴ A similar correlation has been found for oxide interfaces with Si-Ge alloys.³⁴ Evolution kinetics for surface transformations with continuous distributions of activation energies have been studied in detail, particularly for gas desorption, and are known to exhibit abnormally low effective activation energies.³⁵ As temperature increases, excitation of slightly higher-energy states coupled with completion of transformation in slightly lower energy states conspire to attenuate the temperature dependence of the aggregate rate. Weakened temperature dependences give rise to lower effective activation energies. Such effects probably also explain the abnormally low activation energy for defect annihilation in bulk Si damaged by ion implantation,³⁶ wherein local lattice rearrangement (of indeterminate but probably variable type) has been cited as the probable healing mechanism.

C. Coupling to bulk dopant motion

Band bending at the defected interface (or at a clean surface) provides a means by which interface defects can couple to charged point defects in the underlying semiconductor, influencing their motion. Examples of such defects include interstitial silicon, which can exist as Si^{2+} , Si^0 , and Si^- ,³⁷ and interstitial dopants such as boron, which can exist as B_i^+ , B_i^0 , and B_i^- ,³⁸ and as complexes $(\text{B-Si})^+$, $(\text{B-Si})^0$, and $(\text{B-Si})^-$.^{39,40} For p -type doping, interstitial atoms of B and Si are positively charged. The field points into the bulk as shown schematically in Fig. 6 and therefore tends to repel the interstitials from the interface.

The magnitude of this repulsive effect can be estimated as follows. At large doping levels ($>10^{20} \text{ cm}^{-3}$) characteristic of many CMOS device processing applications, the space-charge region in the semiconductor is nominally just a few nanometers wide. At these high carrier concentrations, its depth will vary with position because of the random distribution of dopants as discussed above. Despite this variation,

the magnitude of the average electric field \mathcal{E} in this region can be very roughly approximated from well-known mean-field expressions and is quite large: 2×10^6 V/cm. This field introduces a drift component to the interstitial flux J in addition to the diffusive component according to

$$J = -D \frac{\partial N}{\partial x} + z\mu N \mathcal{E}(x) \approx -D \frac{\Delta N}{\Delta x} + z\mu N \mathcal{E}(x) \quad (3)$$

where N represents the concentration of interstitials, D the corresponding diffusivity, and z the charge. The carrier mobility μ can be approximated roughly (since the semiconductor is degenerate) as qD/kT . In the limit that the interface approximates a “perfect” sink, so that N decreases to zero, ΔN approaches N . Equation (3) can then be rewritten as

$$\begin{aligned} J &\approx -D \frac{\Delta N}{\Delta x} + \frac{zD}{kT} N \mathcal{E}(x) \\ &= \left(-\frac{D}{\Delta x} + \frac{zD}{kT} \mathcal{E}(x) \right) N \\ &= (-A + zB)DN. \end{aligned} \quad (4)$$

For a band bending of ~ 0.5 eV, the drift-related parameter B in Eq. (4) exceeds the diffusion-related parameter A by more than an order of magnitude even at temperatures approaching 1000°C .

Thus, the field is sufficiently strong to virtually stop the motion of positively charged B and Si interstitials toward the interface. (An analogous effect would be observed for negatively charged defects diffusing in n -type material.) The opposing field transforms the interface from a significant sink into a good reflector. Note that this rough treatment represents a conservative estimate. The Si-SiO₂ interface provides a significant, but not perfect, sink for free interstitials,⁴¹ meaning that $\Delta N < N$. Under these conditions, the dominance of drift over diffusion becomes even more accentuated.

Thus, the defects at the interface can couple to the motion of charged defects in the underlying bulk by setting up a space-charge region very close to the interface that strongly repels the bulk defects. One way to represent this repulsion is through the effective interface boundary condition for the diffusion equation describing charged bulk defects. The strong repulsion in the near-interface region in effect makes the boundary condition more reflecting, thereby changing the concentration profile of the bulk defects. In situations wherein these defects mediate diffusion of impurities or other species within the bulk, this change in profile inevitably induces a corresponding change the concentration profile of the mediated species, which in turn leads to modified bulk material properties.

D. Implications for CMOS device processing

These considerations have direct relevance for the formation of p - n junctions in field-effect transistors. Junctions are

typically created by ion implantation of dopants through a thin layer of SiO₂ (Ref. 42) followed by heating to 1000 – 1100°C for 1 s or less to remove implantation damage and electrically activate the dopant. However, much research has shown⁴³ that bulk defects created by implantation mediate rapid dopant diffusion during annealing, which substantially deepens the junction (particularly for boron) and degrades subsequent device performance. A great deal of effort has sought to minimize this “transient-enhanced diffusion,” with the effort guided by detailed modeling of the diffusion of the various point defects and the reactions among them.^{44,45}

Extrapolation of the kinetic data presented here to the temperature range of processing interest shows that implantation-induced band bending persists throughout the annealing step. The corresponding loss of an important interfacial sink for interstitials (particularly of Si) should increase the average concentration of interstitials deeper in the bulk. This increase speeds the rate of kick-in and kick-out reactions between the interstitials and dopant atoms residing in substitutional lattice sites, thereby increasing the net mobility of the dopant. The enhanced mobility inevitably leads to an undesired increase in the depth of the junction, which in current advanced devices lies a few tens of nanometers below.⁴⁶

This scenario suggests that one previously unrecognized limitation to obtaining shallower junctions and correspondingly improved device performance is implantation-induced band bending. Processing methods aimed at reducing band bending after implantation should lead to larger rates of interstitial incorporation at the interface, thereby resulting in shallower junctions.

IV. CONCLUSION

The results presented here point to a previously unrecognized way in which electrically active surface defects can influence the motion of charged mobile species in the underlying bulk. Such motion can determine the material properties of the bulk (such as doping profile after device processing). Coupling of this sort is likely to become increasingly important as semiconductor devices of all sorts shrink to smaller sizes, so that surface and interfaces lie close to the active regions of the devices. The present work has offered an example of how physical and thermal means might be used in tandem to avoid unwanted dopant motion. However, it is easy to envision greatly expanded possibilities for controlling such coupling by adding chemical means to the arsenal for modifying surface and interface defects, and by focusing not only an avoidance but also on the proactive tailoring of material properties in the confined spaces of new generations of devices.

ACKNOWLEDGMENTS

This work was partially supported by NSF (Grants No. CTS 98-06329 and No. CTS 02-03237).

- *Author to whom correspondence should be addressed. Email address: eesebaue@uiuc.edu
- ¹D. Castellanos, H. A. Farach, R. J. Creswick, and C. P. Poole, Jr., *Phys. Rev. B* **47**, 5037 (1993).
 - ²A. M. Mariz, U. M. S. Costa, and C. Tsallis, *Europhys. Lett.* **3**, 27 (1987).
 - ³G. J. Mata, E. Pestana, and M. Kiwi, *Phys. Rev. B* **26**, 3841 (1982).
 - ⁴A. Poniewierski and A. Samborski, *Phys. Rev. E* **53**, 2436 (1996).
 - ⁵L. David, J. Bernard, M. Orrit, and P. Kottis, *Chem. Phys.* **132**, 31 (1989).
 - ⁶F. Baumberger, T. Greber, and J. Osterwalder, *Phys. Rev. B* **62**, 15 431 (2000).
 - ⁷I. M. Vitomirov, G. D. Waddill, C. M. Aldao, S. G. Anderson, C. Capasso, and J. H. Weaver, *Phys. Rev. B* **40**, 3483 (1989).
 - ⁸D. E. Aspnes, *Surf. Sci.* **132**, 406 (1983).
 - ⁹M. McEllistrem, G. Haase, D. Chen, and R. J. Hamers, *Phys. Rev. Lett.* **70**, 2471 (1993).
 - ¹⁰D. E. Aspnes, *Surf. Sci.* **37**, 418 (1973).
 - ¹¹M. Cardona, K. L. Shaklee, and F. H. Pollak, *Phys. Rev.* **154**, 696 (1967).
 - ¹²C. R. Carlson, W. F. Buechter, F. Che-Ibrahim, and E. G. Seebauer, *J. Chem. Phys.* **99**, 7190 (1993).
 - ¹³R. Ditchfield, D. Llera-Rodriguez, and E. G. Seebauer, *Phys. Rev. B* **61**, 13 710 (2000).
 - ¹⁴P. Lautenschlager, M. Garriga, L. Vina, and M. Cardona, *Phys. Rev. B* **36**, 4821 (1987).
 - ¹⁵R. P. Southwell, M. A. Mendicino, and E. G. Seebauer, *J. Vac. Sci. Technol. A* **14**, 928 (1996).
 - ¹⁶H. Z. Massoud, J. D. Plummer, and E. A. Irene, *J. Electrochem. Soc.* **132**, 2685 (1985).
 - ¹⁷H. Shen, S. H. Pan, Z. Hang, J. Leng, F. H. Pollak, J. M. Woodall, and R. N. Sacks, *Appl. Phys. Lett.* **53**, 1080 (1988).
 - ¹⁸T. Kanata, M. Matsunage, H. Takakura, Y. Hamakawa, and T. Nishino, *Jpn. J. Appl. Phys., Part 1* **68**, 5309 (1990).
 - ¹⁹X. Yin, H. M. Chen, F. H. Pollak, Y. Chan, P. A. Montano, P. D. Kirchner, G. D. Pettit, and J. M. Woodall, *J. Vac. Sci. Technol. A* **10**, 131 (1992).
 - ²⁰H. Shen and M. Dutta, *J. Appl. Phys.* **78**, 2151 (1995).
 - ²¹C. R. Lu, R. Anderson, D. R. Stone, W. T. Beard, R. A. Wilson, T. F. Keuch, and S. L. Wright, *Phys. Rev. B* **43**, 11 791 (1991).
 - ²²A. Badakhshan, C. Durbin, C. R. Glosser, K. Alavi, and R. Pathak, *J. Vac. Sci. Technol. B* **11**, 169 (1993).
 - ²³A. Fujimoto, H. Katsumi, M. Okuyama, and Y. Hamakawa, *Jpn. J. Appl. Phys., Part 1* **34**, 804 (1995).
 - ²⁴F. J. Himpsel, P. Heimann, T.-C. Chiang, and D. E. Eastman, *Phys. Rev. Lett.* **45**, 1112 (1980).
 - ²⁵F. G. Allen and G. W. Gobeli, *Phys. Rev.* **127**, 150 (1962).
 - ²⁶F. J. Himpsel, G. Hollinger, and R. A. Pollak, *Phys. Rev. B* **28**, 7014 (1983).
 - ²⁷H. H. Mueller and M. Schulz, *J. Mater. Sci.* **6**, 65 (1995).
 - ²⁸K. L. Brower, *Appl. Phys. Lett.* **43**, 1111 (1983).
 - ²⁹A. Stesmans, *Phys. Rev. B* **48**, 2418 (1993), and references therein.
 - ³⁰D. L. Griscom, *J. Appl. Phys.* **58**, 2524 (1985).
 - ³¹A. Stesmans, *Appl. Phys. Lett.* **68**, 2076 (1996).
 - ³²A. Stesmans, *Physica B* **273-274**, 1015 (1999).
 - ³³J. C. C. Tsai, in *VLSI Technology* (McGraw-Hill, New York, 1983).
 - ³⁴F. J. Himpsel, F. R. McFeely, A. T-Ibrahimi, and J. A. Yarmoff, *Phys. Rev. B* **38**, 6084 (1988).
 - ³⁵E. G. Seebauer, *Surf. Sci.* **316**, 391 (1994); E. G. Seebauer, A. C. F. Kong, and L. D. Schmidt, *ibid.* **193**, 417 (1988).
 - ³⁶C. Christofides, *Semicond. Sci. Technol.* **7**, 1283 (1992).
 - ³⁷W.-C. Lee, S.-G. Lee, and K. J. Chang, *J. Phys.: Condens. Matter* **10**, 995 (1998).
 - ³⁸G. D. Watkins, *Phys. Rev. B* **12**, 5824 (1975).
 - ³⁹W. Windl, M. M. Bunea, R. Stumpf, S. T. Dunham, and M. P. Masquelier, *Phys. Rev. Lett.* **83**, 4345 (1999).
 - ⁴⁰M. Hakala, M. J. Puska, and R. M. Nieminen, *Phys. Rev. B* **61**, 8155 (2000).
 - ⁴¹H.-H. Vuong, C. S. Rafferty, S. A. Eshraghi, J. Ning, J. R. McMacken, S. Chaudhry, J. McKinley, and F. A. Stevie, *J. Vac. Sci. Technol. B* **18**, 428 (2000).
 - ⁴²This thin layer is commonly termed a "screen oxide."
 - ⁴³S. C. Jain, W. Schoemaker, R. Lindsay, P. A. Stolk, S. Decoutere, M. Willander, and H. E. Maes, *J. Appl. Phys.* **91**, 8919 (2002), and references within.
 - ⁴⁴*Rapid Thermal Processing: Science and Technology*, edited by R. B. Fair (Academic, Boston, 1993).
 - ⁴⁵See, for example, *Si Front-End Processing: Physics and Technology of Dopant-Defect Interactions*, edited by H.-J. L. Gossmann, T. E. Haynes, M. E. Law, A. N. Larsen, and S. Odanaka, MRS Proc. No. 568 (Materials Research Society, Warrendale, PA, 1999); *Si Front-End Processing: Physics and Technology of Dopant-Defect Interactions II*, edited by A. Agarawal, L. Pelaz, H.-H. Vuong, P. Packan, and M. Kase, MRS Proc. No. 610 (Materials Research Society, Warrendale, PA, 2000).
 - ⁴⁶N. E. B. Cowern, J. T. F. Janssen, and H. F. F. Jos, *J. Appl. Phys.* **68**, 6191 (1990).